

1 *Article*

## 2 **Direct Infusion Targeted Metabolomics of Phytochemicals in a Drought** 3 **Tolerant Plant Introduction Soybean Cultivar**

4 **Kevin J. Zemaitis<sup>1</sup>, Heng Ye<sup>2</sup>, Henry T. Nguyen<sup>2</sup>, and Troy D. Wood<sup>1,\*</sup>**

5 <sup>1</sup> Department of Chemistry, Natural Sciences Complex, University at Buffalo, State University of New York, Buffalo,  
6 NY 14260, USA

7 <sup>2</sup> Division of Plant Sciences and National Center for Soybean Biotechnology, University of Missouri, Columbia, MO  
8 65211, USA

9 \* Correspondence: Troy D. Wood, Email: twood@buffalo.edu

---

### 10 **ABSTRACT**

11 Drought is the most prolific form of abiotic stress that legumes and cereal plants alike can endure; planting  
12 of an improper cultivar at the beginning of a season can cause unexpected losses up to fifty-percent under  
13 water deficient conditions. Herein, a plant introduction (PI) of an exotic cultivar of soybean (*Glycine max*),  
14 *PI 567731*, which demonstrates a slow wilting canopy phenotype in maturity group III was profiled in  
15 drought stress field trials in Missouri against a drought susceptible check cultivar, *Pana*. Relative  
16 phytochemical content of chlorophyll (chl) a/b, and pheophytin (pheo) was profiled by direct infusion  
17 electrospray Fourier transform ion cyclotron resonance (FT-ICR) mass spectrometry. High-throughput  
18 detection of metabolic profiles in twenty-four experimental groups occurred in triplicate within a few hours,  
19 without chromatographic separation. Subsequent multivariate analysis was able to form predictive models,  
20 encompassing the variance of growth and drought stress, within the experimental groupings at two  
21 physiological ages. Statistically significant increases within the Chl content in control conditions were  
22 detected, and an expanded photosynthetic antenna within the drought affected treatment condition could  
23 account for increased photosynthetic content; in particular, the distinct enhancement of chl b is noted from  
24 *PI 567731*. Moreover, the existence of unique chl-related metabolites ( $m/z > 900$ ) were confirmed through  
25 tandem mass spectrometry. The resultant coordination of fatty acids to the core of the porphyrin ring plays  
26 an unknown role in the proliferation of the photosynthesis, however the relative ratio of the most abundant  
27 chl-related metabolite is undisturbed by drought stress in *PI 567731*, in contrast to the drought susceptible  
28 cultivar.

29 **KEYWORDS:** plant introduction, drought stress response, slow wilting canopy, drought tolerance,  
30 chlorophyll content, phytochemicals, soybean, direct infusion, FT-ICR, metabolomics

### 31 **ABBREVIATIONS**

32 PI, plant introduction; SW, slow canopy wilting; MG, maturity group; QTL, quantitative trait loci; RIL,  
33 recombinant inbred line; Chl, chlorophyll; Pheo, pheophytin; GC/LC, gas or liquid chromatography; NMR,  
34 nuclear magnetic resonance; FT-ICR, Fourier transform ion cyclotron resonance; MS, mass spectrometry; DI,

35 direct infusion; ESI, electrospray ionization; CID, collision induced dissociation; 3D, three-dimensional; PCA,  
36 principal component analysis; PLS-DA, partial least squares discriminant analysis; ODT, old drought treated;  
37 OC, old control; YDT, young drought treated; YC, young control

## 38 INTRODUCTION

39 Agricultural crops can endure a matrix of stress resultant from a variety of sources including biotic or  
40 abiotic stressors such as drought, flooding, salinity, or nutrient availability [1]. Among the different sources  
41 of stress plants can undergo, varying levels of water deficiency and drought have the most prolific and  
42 detrimental effect to agricultural farms on the global and national scale [2]. Numerous plant traits have  
43 been identified for the potential of improving the performance of drought-affected crops, mainly through  
44 conservation of water [3], with more recent works identifying the importance of slow canopy wilting (SW)  
45 phenotypes for their potential stress tolerance in water deficient environments [4]. Legumes, such as  
46 soybean (*Glycine max*), have a particular intolerance to water deficiency in the early stages of growth and  
47 flowering, where a decrease in water availability by half can result in up to a loss of half the expected yields  
48 [5]. Persistent changes in climate are predicted to have further detrimental impacts on agriculture in the  
49 coming decades [6].

50 Recently, an exotic soybean germplasm, *plant introduction (PI) 567731* in maturity group III (MG III), was  
51 identified to consistently express the SW phenotype in the field compared to the drought sensitive cultivar  
52 *Pana* [4,7]. *PI 567731* showed lower yield loss than *Pana* under drought stress with greater than 13% more  
53 yield index (yield under rain-fed/ yield under irrigation) [7]. *PI 567731* was found to use significantly less  
54 water under drought conditions, and this water conservation strategy was identified to be associated with  
55 limited-maximum transpiration rates. The transpiration of *PI 567731* was found to be sensitive to an  
56 aquaporin inhibitor (silver-nitrate) indicating the independence of a limited-maximum transpiration to a  
57 lack of silver-sensitive aquaporins in these SW genotypes. A major SW quantitative trait loci (QTL)  
58 (*qSW\_Gm10*) was mapped on chromosome 10 from *PI 567731* through a genetic study in a recombinant  
59 inbred line (RIL) population and this QTL was further confirmed to delay canopy wilting under drought  
60 conditions in a near-isogenic background [4].

61 In efforts to understand many findings from field trials and further mapping of QTLs, many researchers  
62 have adopted use of proteomic and metabolomic techniques and platforms for data analysis to further  
63 reinforce and probe the mechanisms of plant stress responses. As resultant responses are characteristic to  
64 either acute or prolonged effects to drought stress, the initial impacts primarily effect net photosynthesis  
65 and photosynthetic performance of the plants. Under drought stress, stomatal closures and hormonal  
66 signaling through abscisic acid have been identified as the key reductants to net photosynthesis [8], with  
67 increased efficiency of the photosystem (PS) II denoted in stress tolerance [9]. Extended periods of drought  
68 stress have been demonstrated to also induce reduced Chlorophyll (Chl) content and related fluorescence

69 parameters [10], and are critical in considerations of the photosystem (PS) II, with drought stress also having  
70 noted to induce reordering the PSII core [11]. Even though water deficiencies do not directly impact the  
71 primary components of C3 plants PSI or PSII directly, these secondary impacts are well known in a variety  
72 of crops to reversibly impact photosynthesis, prior to photosynthetic decay [12]. This emphasizes the need  
73 for targeted approaches of profiling phytochemicals as a reliable means of screening for stress tolerances,  
74 including drought tolerance [13,14].

75 Both targeted and non-targeted approaches for determining metabolic profiles of soybean, and other  
76 agronomical crops have been entailed with instrumental approaches ranging from gas or liquid  
77 chromatography (GC/LC) coupled with mass spectrometry (MS) [15,16], nuclear magnetic resonance (NMR)  
78 [17,18], and a variety of spectroscopic techniques for in-vivo studies [9]. No one all-inclusive method for  
79 simultaneous detection of all metabolites is available. With a broad array of expression in a variety of  
80 primary and secondary metabolites in model plants and agricultural crops, methods either prove to be  
81 either moderate throughput with high specificity in extracts, or lack specificity with high-throughput  
82 analysis. High-resolution accurate mass MS platforms such as Fourier Transform ion cyclotron resonance  
83 (FT-ICR), due to unprecedented mass resolving power and mass accuracy [19], allows for the direct infusion  
84 of samples with no on-line separations [20]. In comparison to other MS profiling techniques, direct infusion  
85 FT-ICR holds at least a ten-fold decrease in analysis time, while simultaneously detecting hundreds of  
86 metabolic signals. As such, the platform is ideal for determination of relative phytochemical content. When  
87 utilized in tandem with physiological data and other interconnected pathways, insight on the  
88 acclimatization of photosynthesis in stress tolerances can be gleaned [21]. Herein described is the targeted  
89 profiling of phytochemical content and multivariate analysis of a drought tolerant cultivar, *PI 567731*, in  
90 comparison to a drought susceptible cultivar, *Pana*, grown in field trials, with drought treatment consisting  
91 of no irrigation or rainfall for three weeks.

## 92 MATERIALS AND METHODS

### 93 Materials

94 Quinapril HCl used was a USP Reference Standard (Rockville, MD). Methanol (HPLC Grade) was from Sigma-  
95 Aldrich (St. Louis, MO), and formic acid 88% (Certified ACS) was from Fisher Scientific (Fair Lawn, NJ)  
96 Whatman (Cat. 1001-055) filtration papers were used for vacuum filtration of particulate matter.

### 97 Samples Used During the Study

98 Two cultivars of soybean (*Glycine max*), *PI 567731* and *Pana*, were grown in field trials at the University of  
99 Missouri (latitude 38.895305, longitude -92.205917). Two sets of the two soybean lines were grown in the  
100 field 20 meters away from each other under well-watered conditions. Sample collection was completed for

101 each of the two sets after 3 weeks without rain in the field. One set was irrigated 2 days prior to sample  
102 collection, which was considered as a control condition. The other set did not receive water either from rain  
103 or irrigation for 3 weeks, which was considered as drought condition. Leaf samples were collected at two  
104 physiological stages: young at V5 growth stage and old at R2 growth stage. After collection, leaves were flash  
105 frozen and transported at -80°C, and stored in polycarbonate petri-dishes at -20°C until extractions were  
106 processed.

### 107 **Metabolite Extraction Protocol**

108 The experimental and control groups underwent a respective pooling of plant tissue from the leaves  
109 collected. The samples were flash frozen with liquid nitrogen and macerated in an aliquot of solvent with  
110 an internal standard added. Maceration continued for five minutes and particulate matter was subsequently  
111 removed through vacuum filtration. Samples were dried in a vacuum oven at ambient temperatures and  
112 diluted to constant volume.

### 113 **Data Collection and Processing**

114 All spectra were acquired on a dual-source Bruker Daltonics 12T Solarix FT-ICR mass spectrometer  
115 (Bremen, Germany) by DI electrospray ionization (ESI) of the samples. Datasets for multivariate analysis  
116 were collected at 2 Mw using broadband detection from  $m/z$  147.4 to 1500 with 100 scans for a transient of  
117 0.8389 sec. Solvent extracts were analyzed in triplicate for instrumental and technical replicates of the two  
118 cultivars for both experimental conditions. Spectra were processed in DataAnalysis 5.0 with a signal-to-noise  
119 ratio of 5.0 for peak picking. Collision induced dissociation (CID) was used to confirm the identity of Chl-  
120 related metabolites, no charging additives were added due to sufficient signal in positive ionization mode.  
121 To reduce complex adduction, 0.1% of formic acid (v/v) was added during CID experiments at 4 Mw for a  
122 transient of 1.6778 sec with sufficient number of scans.

### 123 **Statistical Analysis of Metabolites**

The online web platform MetaboAnalyst 5.0 (<https://www.metaboanalyst.ca/>) was used for statistical analysis [22], and METLIN (<https://metlin.scripps.edu/>) was used for metabolite annotation [23]. Within MetaboAnalyst 5.0, a window of 2.5mDa was used to bin peaks from technical and instrumental replicates by DI FT-ICR MS. Peaks within samples with greater than 80% missing values were removed, and missing values were imputed utilizing an estimated limit of detection (one-fifth the average signal) for missing values. For multivariate analysis, filtering based upon standard deviation was completed, and normalization was completed to the peak area of the internal standard to remove variance from DI-ESI. Log fold changes were generated through transformation of the data.

## RESULTS AND DISCUSSION

### Multivariate Analysis of Cultivar Treatments

Principal component analysis (PCA) was performed as an orthogonal model to partial least squares discriminant analysis (PLS-DA) in order to discriminate subsets of drought treatment in the cultivars in MetaboAnalyst 5.0. Shown in Figure 1 are the three dimensional (3D) PCA of the entire sample population and models segmented according to the cultivar. This was completed to identify outliers initially from the 72 samples, with an average of 2,560 peaks per sample, after which further analysis was completed. The models demonstrate the distinct variance in the datasets from the control and drought treated metabolic fingerprints, as well as the unique variance to each cultivar, allowing for the distinction amongst the DI FT-ICR MS datasets.

Alongside of the drought treatment, the extra period of growth was also incorporated into the study to identify the influence of growth on the soybean plants. As shown in

Figure 2A and 2B within PLS-DA models, the variance of growth was able to be separated. For the young

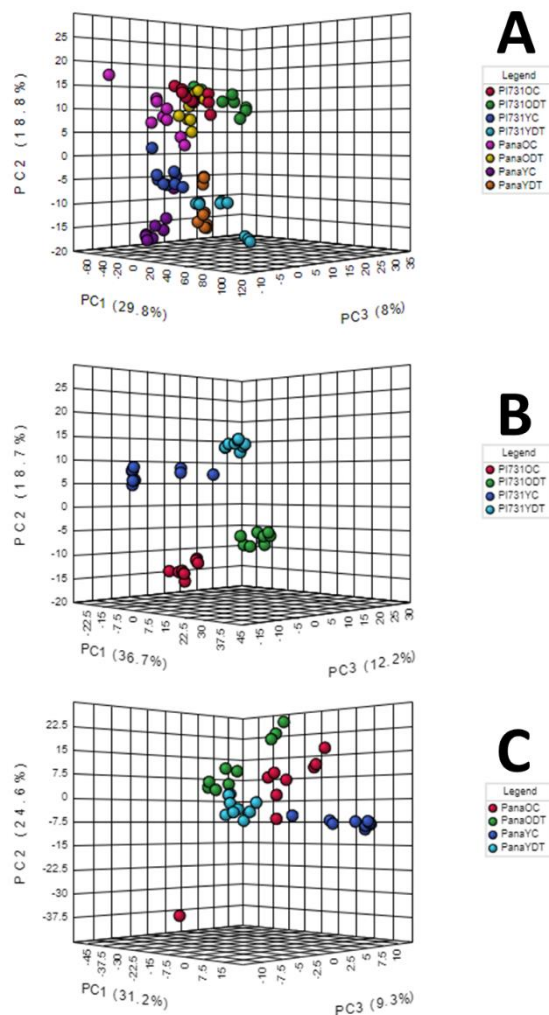


Figure 1. (A) is a 3D scores plot of the PCA of all *Pana* and *PI 567731*, (B) is the 3D-PCA of all *PI 567731* datasets, and (C) is the 3D-PCA of all *Pana* datasets. Each legend is unique to each scores plot, and is to the right of each plot.

control (YC) and young drought treated (YDT) samples, the first component encompassed variance which separates the datasets, and the third component encompassed the variance imposed by drought itself based upon the groupings. These analyses utilize 95% confidence intervals in the scores plots, in the form of ellipses surrounding each subset population, allowing for the visual investigation of the analysis of variance between models. From the first component of the PLS-DA (Fig.2A, 2C), *Pana* datasets within the model had greater variance explained overall as well as both cultivars were distinguished by physiological age grouping. The third component of the model (Fig.2B, 2D), demonstrates overlapping confidence intervals in the case of *PI 567731*, with less

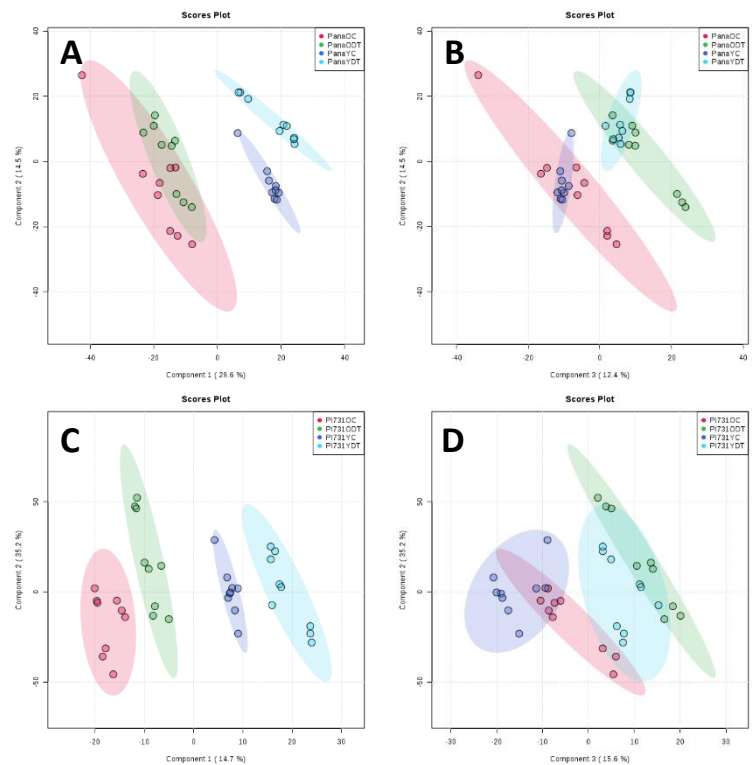


Figure 2. PLS-DA score plots of the first and second components (A, C) and the second and third components (B, D) of all subsets of *Pana* (A, B) and *PI 567731* (C, D) samples. With a window of 95% confidence around the encompassed variance.

observable variance within the metabolic fingerprint for both YDT/ODT, having compositions closer to that of the YC/OC in the third component. PLS-DA is the most commonly implemented tool in metabolomics datasets for a multitude of reasons; however, caution must be utilized with the raw data matrix, as the groupings can lead to a tendency to over fit the model when a variety of factors are not considered[24]. Based upon comparisons to the PCA, and other measures within MetaboAnalyst, this was not observed; as to not impart effects of growth on the further targeted analysis, OC/ODT were further analyzed independent of the YC/YDT datasets.

### Profiling Chlorophyll Content in the Treatments

*PI 567731* was identified to preserve soil water through limited-maximum transpiration rates; this behavior would ultimately result in increased stomatal closures throughout the plant's life cycle, and decreased photosynthesis. Electron transport rates, carboxylation rates, respiration rates, and intrinsic water use efficiencies follow the dependencies of increased stomatal closures exhibited in water deficient events, with photosynthetic decay only occurring over extended periods of stress [25,26]. Throughout the profiling of the OC/ODT and YC/YDT datasets, it was observed that increased levels of Chl a/b, and Pheophytin (Pheo) were

187 observed to be statistically enhanced  
 188 components within the samples of *PI*  
 189 *567731*, with an overall median  
 190 increase in relative abundance of  
 191 Pheo a and Chl b detected within *PI*  
 192 *567731* as shown in the box and  
 193 whisker plots in Figure 3.

194 T-tests were conducted for individual  
 195 adducts for treatments of *Pana* and  
 196 *PI 567731*. *PI 567731* OC was found to  
 197 have statistically significant log fold  
 198 increases ( $p \leq 0.05$ ) for the sodiated  
 199 adduct Chl b ( $p = 0.010$ ) and Pheo a ( $p$   
 200  $= 0.0006$ ), as well as the protonated  
 201 Pheo a ( $p = 0.033$ ) in reference to  
 202 *Pana* OC. Sodiated Chl b content was  
 203 found to be significantly enhanced in  
 204 *PI 567731* ODT ( $p = 0.039$ ) in reference  
 205 to *Pana* ODT. Distributions for the  
 206 YC/YDT found significance for the

207 protonated Chl a ( $p = 0.0005$ ) in the YC of *PI 567731* and protonated form of Pheo a ( $p = 0.019$ ) in the YDT of  
 208 *PI 567731* over the corresponding *Pana* OC/ODT trials. These individual adducts account for the log fold  
 209 distributions within the binned peak areas shown in the OC/ODT and YC/YDT plots in Figure 3, with most  
 210 Pheo a levels remaining consistent, with highlights of elevated levels of Chl b for *PI 567731*.

211 The average abundances and ratio of these metabolites has previously been demonstrated as secondary  
 212 links to the holistic health of the plant, as demonstrated in previous works on Chl and related metabolites  
 213 as markers for stress tolerance [27]. Increased total chlorophyll content was observed to be statistically  
 214 significant by ANOVA ( $p \leq 0.05$ ); previously this has been observed within positive chilling tolerance  
 215 responses in maize [28]. With the noted increased yield index from the PI, alongside the QTL SW phenotypic  
 216 expression, this increase in total chlorophyll content is indicative that chlorophyll content is up-regulated  
 217 when the SW MGIII cultivar experiences drought stress, especially in earlier stages of growth. The  
 218 observable enhancement was maintained under the drought treatment in younger populations of leaves,  
 219 signifying that the three weeks of drought treatment with subsequent irrigation did not cause degradation,  
 220 however it did cause a shift to the average Chl a/b ratios.

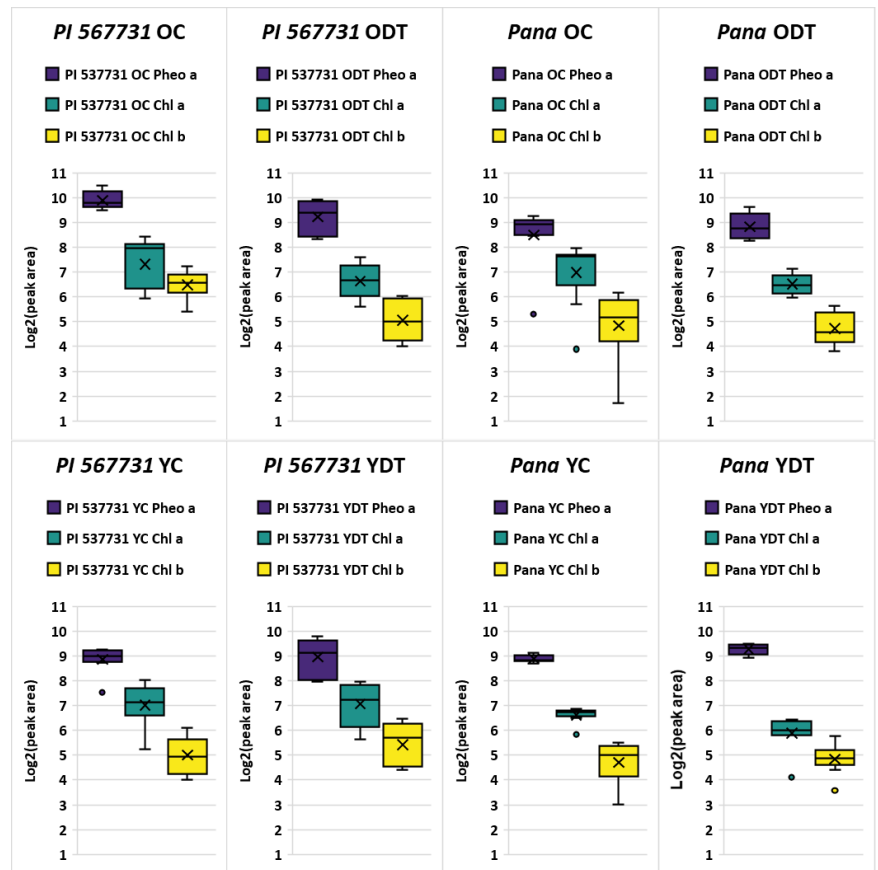


Figure 3. General log scale box and whisker plots of the binned protonated and sodiated adducts from *Pana* and *PI 567731* for Pheo a, and Chl a/b for OC, ODT, YC, and YDT. The solid black line represents the median, and black X represents the mean peak area for all subsets.

The enhanced expression of Chl b relative to *Pana* also marks proliferation of the photosystem, in agreement with increasing the breadth of the photosynthetic antennae in plants with positive stress responses [29]. The decrease within *PI 567731* for Chl b is also indicative of drought stress responses, while still remaining consistent with the drought susceptible control levels of *Pana* when *PI 567731* is under drought stress during later stages of growth. Within studies of maize and rice, with known water deficient intolerances, the photosynthetic antenna has been shown to be broadened, and an altered ratio of Chl a/b within tolerant cultivars is observed [30]. It has also been demonstrated Chl b is not just an accessory pigment in the light harvesting system, and can play a more pertinent role in primary light harvesting complexes [29], possibly allowing for more efficient use of light despite limited-maximum transpiration rate within earlier stages of growth. Moreover, the relative content should be at the same level of physiological responses from *Pana* if there was no existence of a positive stress response enhanced by a broadened photosynthetic antenna. The mapping of the SW QTL on chromosome 10 further suggests that in times of stomatal openings these increased levels of Chl content in the PI allow for efficient photosynthesis.

#### Tandem Mass Spectrometry of Novel Chlorophyll Related

While further profiling the annotated metabolites, distinct novel Chl-related metabolites previously reported within soybean extracts were also denoted within this research, highlighted by Chl-related metabolite at  $m/z$  1073.70740 [31]. As shown in the box and whisker plot in Figure 4, general log fold increases are experienced comparing young to older populations, with an increased median expression in drought treatment of the susceptible cultivar *Pana*. However, *PI 567731* levels of this sodium adduct remain relatively stable through drought stress response. Through the fragmentation of the molecules by collision induced dissociation (CID), these species (>893 Da) showed characteristic losses to that of a porphyrin ring base. Distinct moieties attached directly to the porphyrin ring are apparent by the neutral losses from the precursor ion, which still exhibits characteristic

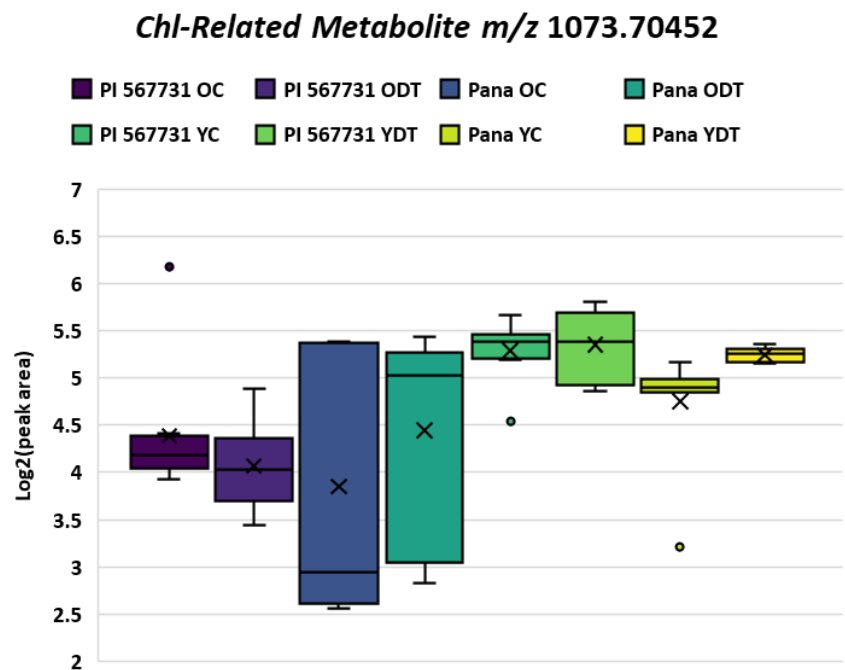


Figure 4. Box and whisker plot of Chl-related metabolite at  $m/z$  1073.70483 relative log scale abundance in both *Pana* and *PI 567731* in both OC/ODT and YC/YDT datasets, legend above.



253 loss of the phytol group ( $C_{20}H_{38}$ ), as  
254 shown in the spectrum in Figure 5.

255 Once isolated, a product ion at  
256 893.55473 Da forms, corresponding to a  
257 sodium adduct of Pheo a through the  
258 neutral loss of 180.15031 Da. When a  
259 neutral loss search within METLIN is

260 completed with annotation in LIPID  
261 MAPS, this yields matches with a  
262 conjugated fatty acid ( $C_{12}H_{20}O$ ). Upon  
263 further fragmentation, neutral losses of

264 278.29692 Da and 76.01606 Da appear, as annotated in Table 1, corresponding to the loss of the phytol group  
265 ( $C_{20}H_{38}$ ) to pheophorbide a, and further loss of moieties on the porphyrin ring ( $C_2H_5O_3$ ), respectively. These  
266 results are consistent with previously reported literature studies of fragmentation of both Chl a and Pheo a  
267 by various dissociation techniques on FT-ICR MS [32,33]. A generation of a neutral loss under weak  
268 collisional energies (and the loss of an intact phytol) suggests a weak coordination or bond formed to the  
269 porphyrin ring, not a modification that is not directly linked to the phytol group. However, fractionation  
270 and NMR will be needed to confirm the fragmentation results.

271 Literature reports have noted increased fatty acid and lipid content within mesophyll membranes and  
272 chloroplasts to be essential for various stress tolerances [34], and are postulated to be pertinent to regulation  
273 of chloroplasts, especially under low or high temperatures, and abiotic stress [35,36]. This has a further

274 influence upon Chl-protein  
275 complexes, with heterogeneous lipid  
276 and fatty acid composition of the  
277 membranes. With various Chl-  
278 related metabolites (>893 Da) being  
279 reported, fragmentation does  
280 confirm relation to Chl and Pheo in  
281 the porphyrin metabolism for these  
282 metabolites due to characteristic  
283 neutral losses; however, the  
284 metabolic pathway for the  
285 attachment and position on the  
286 porphyrin ring is unknown.

Molecular Formula	Theoretical Mass	Observed Mass	Mass Error (ppm)
$C_{67}H_{94}N_4O_6Na$	1073.70656	1073.70483	1.61
$C_{55}H_{74}N_4O_5Na$	893.55514	893.55450	0.64
$C_{49}H_{64}N_4O_4Na$	795.48198	795.48019	2.21
$C_{35}H_{36}N_4O_5Na$	615.25779	615.25804	-0.40
$C_{33}H_{32}N_4O_2Na$	539.24175	539.24168	0.12

Table 1. Molecular formula, theoretical mass, observed mass, and calculated mass error in ppm for the precursor and fragment ions from the CID of chlorophyll related metabolite at  $m/z$  1073.70483 with 30eV of collisional energy with argon as the collision gas.

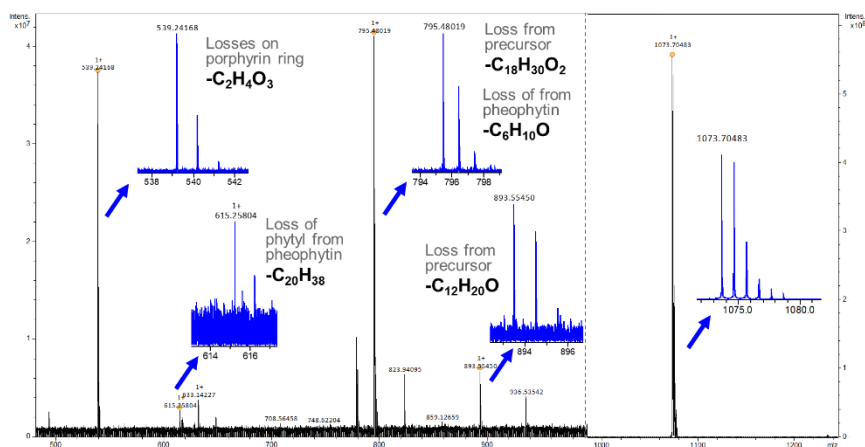


Figure 5. CID of chlorophyll related metabolite at  $m/z$  1073.70483 at 30eV with argon collision gas, the precursor y-axis scale is  $\times 10^8$  where fragment ions scale is  $\times 10^7$ . Characteristic losses of pheophytin occur with losses highlighted from either the sodiated pheophytin at  $m/z$  893.55514 (0.64 ppm error) or the precursor chlorophyll related metabolite ion at  $m/z$  1073.70483 (1.61 ppm error).

287 Considering that many of the species were also heavily oxidized, as apparent by high resolution accurate  
288 mass annotation of the full scan mass spectrum, this could also be a byproduct of reactive oxygen signaling  
289 (ROS) or of Chl-binding complexes in PSII membranes. Further study of these molecules is warranted.

## 290 CONCLUSIONS

291 Overall, *PI 567731*, a SW phenotype in MGIII with a profiled QTL on chromosome 10, was profiled in  
292 drought stress field trials against *Pana*, a drought susceptible metabolite. Multivariate analysis confirmed  
293 that the flux exhibited by drought stress detected by DI FT-ICR MS in the *PI 567731* was less extensive than  
294 that exhibited by the susceptible cultivar and more comparable to the control, forming predictive models  
295 for future analyses. Statistically significant increases within the Chl content in control conditions were also  
296 detected, and an expanded photosynthetic antenna within the drought affected treatment condition could  
297 account for increased photosynthetic content despite limited-maximum transpiration rates in the SW  
298 phenotype. With prior confirmation of the increased yield index and other physiological measures, profiling  
299 and observing the increased phytochemical content demonstrates the utility of this analysis in concert with  
300 physiological data for obtaining broad and focused profiled of metabolites. Furthermore, novel chlorophyll-  
301 related metabolites were probed within the analysis and confirmed with through tandem mass  
302 spectrometry to have fatty acids attached or coordinated as moieties to the porphyrin ring, with an unknown  
303 mechanism of attachment and relation into the porphyrin metabolism and photosynthesis.

## 304 DATA AVAILABILITY

305 The dataset of the study is available from the authors upon reasonable request.

## 306 AUTHOR CONTRIBUTIONS

307 KJZ, YH, HTN, and TDW conceived and designed experiments, YH raised and harvested plant specimens,  
308 KJZ performed the metabolomic assays using mass spectrometry, KJZ, YH, HTN, and TDW analyzed the data,  
309 KJZ wrote the manuscript, and KJZ, YH, HTN, and TDW revised and finalized the manuscript.

## 310 CONFLICTS OF INTEREST

311 The author(s) declare(s) that they have no conflicts of interest.

## 312 FUNDING

313 The authors gratefully acknowledge funding through the National Institutes of Health National Center for  
314 Research Resources (Grant S10-RR029517-01) used to obtain the dual-source Bruker Daltonics 12T Solarix  
315 FT-ICR mass spectrometer, also the New York Corn and Soybean Growers Association (Grant SYBN 19-002)  
316 and United Soybean Board (Project #1820-172-0130) for the financial support for this research.

## 317 ACKNOWLEDGMENTS

318 The authors gratefully acknowledge the Chemistry Instrument Center at the University at Buffalo for  
319 housing the mass spectrometer used within this study.

## 320 REFERENCES

- 321 1. Pandey P, Irulappan V, Bagavathiannan MV, Senthil-Kumar M. Impact of Combined Abiotic and Biotic Stresses  
322 on Plant Growth and Avenues for Crop Improvement by Exploiting Physio-morphological Traits. *Frontiers in Plant*  
323 *Science*. 2017;8(537).
- 324 2. Lesk C, Rowhani P, Ramankutty N. Influence of extreme weather disasters on global crop production. *Nature*.  
325 2016;529(7584):84-7.
- 326 3. Chaves M, Oliveira M. Mechanisms underlying plant resilience to water deficits: prospects for water-saving  
327 agriculture. *Journal of experimental botany*. 2004;55(407):2365-84.
- 328 4. Ye H, Song L, Schapaugh WT, Ali ML, Sinclair TR, Riar MK, et al. The importance of slow canopy wilting in  
329 drought tolerance in soybean. *Journal of Experimental Botany*. 2020;71(2):642-52.
- 330 5. Frederick JR, Camp CR, Bauer PJ. Drought - stress effects on branch and mainstem seed yield and yield  
331 components of determinate soybean. *Crop science*. 2001;41(3):759-63.
- 332 6. Howden SM, Soussana J-F, Tubiello FN, Chhetri N, Dunlop M, Meinke H. Adapting agriculture to climate  
333 change. *Proceedings of the National Academy of Sciences*. 2007;104(50):19691.
- 334 7. Pathan SM, Lee J-D, Sleper DA, Fritschi FB, Sharp RE, Carter Jr. TE, et al. Two Soybean Plant Introductions  
335 Display Slow Leaf Wilting and Reduced Yield Loss under Drought. *Journal of Agronomy and Crop Science*.  
336 2014;200(3):231-6.
- 337 8. Mutava RN, Prince SJK, Syed NH, Song L, Valliyodan B, Chen W, et al. Understanding abiotic stress tolerance  
338 mechanisms in soybean: A comparative evaluation of soybean response to drought and flooding stress. *Plant*  
339 *Physiology and Biochemistry*. 2015;86:109-20.
- 340 9. Iqbal N, Hussain S, Raza MA, Yang C-Q, Safdar ME, Brestic M, et al. Drought Tolerance of Soybean (*Glycine max*  
341 *L. Merr.*) by Improved Photosynthetic Characteristics and an Efficient Antioxidant Enzyme Activities Under a Split-  
342 Root System. *Front Physiol*. 2019;10:786-.
- 343 10. Dong S, Jiang Y, Dong Y, Wang L, Wang W, Ma Z, et al. A study on soybean responses to drought stress and  
344 rehydration. *Saudi Journal of Biological Sciences*. 2019;26(8):2006-17.
- 345 11. Giardi M, Cona A, Geiken B, Kučera T, Masojidek J, Mattoo A. Long-term drought stress induces structural and  
346 functional reorganization of photosystem II. *Planta*. 1996;199(1):118-25.
- 347 12. Ghotbi - Ravandi A, Shahbazi M, Shariati M, Mulo P. Effects of mild and severe drought stress on  
348 photosynthetic efficiency in tolerant and susceptible barley (*Hordeum vulgare L.*) genotypes. *Journal of agronomy*  
349 *and crop science*. 2014;200(6):403-15.
- 350 13. Li R-h, Guo P-g, Michael B, Stefania G, Salvatore C. Evaluation of Chlorophyll Content and Fluorescence  
351 Parameters as Indicators of Drought Tolerance in Barley. *Agricultural Sciences in China*. 2006;5(10):751-7.
- 352 14. Mafakheri A, Siosemardeh A, Bahramnejad B, Struik P, Sohrabi Y. Effect of drought stress on yield, proline and  
353 chlorophyll contents in three chickpea cultivars. *Australian journal of crop science*. 2010;4(8):580-5.
- 354 15. Das A, Rushton PJ, Rohila JS. Metabolomic Profiling of Soybeans (*Glycine max L.*) Reveals the Importance of  
355 Sugar and Nitrogen Metabolism under Drought and Heat Stress. *Plants (Basel)*. 2017;6(2):21.
- 356 16. Lima LL, Balbi BP, Mesquita RO, Silva JCFd, Coutinho FS, Carmo FMS, et al. Proteomic and Metabolomic  
357 Analysis of a Drought Tolerant Soybean Cultivar from Brazilian Savanna. *Crop Breeding, Genetics and Genomics*.  
358 2019;1(2):e190022.

- 359 17. Barding GA, Jr., Béni S, Fukao T, Bailey-Serres J, Larive CK. Comparison of GC-MS and NMR for metabolite  
360 profiling of rice subjected to submergence stress. *Journal of proteome research*. 2013;12(2):898-909.
- 361 18. Charlton AJ, Donarski JA, Harrison M, Jones SA, Godward J, Oehlschlager S, et al. Responses of the pea (*Pisum*  
362 *sativum* L.) leaf metabolome to drought stress assessed by nuclear magnetic resonance spectroscopy.  
363 *Metabolomics*. 2008;4(4):312.
- 364 19. Shaw JB, Lin T-Y, Leach FE, Tolmachev AV, Tolić N, Robinson EW, et al. 21 Tesla Fourier Transform Ion  
365 Cyclotron Resonance Mass Spectrometer Greatly Expands Mass Spectrometry Toolbox. *Journal of The American*  
366 *Society for Mass Spectrometry*. 2016;27(12):1929-36.
- 367 20. Kirwan JA, Weber RJM, Broadhurst DI, Viant MR. Direct infusion mass spectrometry metabolomics dataset: a  
368 benchmark for data processing and quality control. *Scientific Data*. 2014;1(1):140012.
- 369 21. Pinheiro C, Chaves MM. Photosynthesis and drought: can we make metabolic connections from available  
370 data? *Journal of Experimental Botany*. 2010;62(3):869-82.
- 371 22. Chong J, Wishart DS, Xia J. Using MetaboAnalyst 4.0 for Comprehensive and Integrative Metabolomics Data  
372 Analysis. *Curr Protoc Bioinformatics*. 2019;68(1):e86.
- 373 23. Smith CA, O'Maille G, Want EJ, Qin C, Trauger SA, Brandon TR, et al. METLIN: a metabolite mass spectral  
374 database. *Therapeutic drug monitoring*. 2005;27(6):747-51.
- 375 24. Gromski PS, Muhamadali H, Ellis DI, Xu Y, Correa E, Turner ML, et al. A tutorial review: Metabolomics and  
376 partial least squares-discriminant analysis--a marriage of convenience or a shotgun wedding. *Anal Chim Acta*.  
377 2015;879:10-23.
- 378 25. Medrano H, Escalona JM, Bota J, Gulías J, Flexas J. Regulation of photosynthesis of C3 plants in response to  
379 progressive drought: stomatal conductance as a reference parameter. *Annals of botany*. 2002;89 Spec No(7):895-  
380 905.
- 381 26. Sinclair TR, Hammer GL, van Oosterom EJ. Potential yield and water-use efficiency benefits in sorghum from  
382 limited maximum transpiration rate. *Functional Plant Biology*. 2005;32(10):945-52.
- 383 27. Dalal VK, Tripathy BC. Water-stress induced downsizing of light-harvesting antenna complex protects  
384 developing rice seedlings from photo-oxidative damage. *Scientific Reports*. 2018;8(1):5955.
- 385 28. Waqas MA, Khan I, Akhter MJ, Noor MA, Ashraf U. Exogenous application of plant growth regulators (PGRs)  
386 induces chilling tolerance in short-duration hybrid maize. *Environmental Science and Pollution Research*.  
387 2017;24(12):11459-71.
- 388 29. Kume A, Akitsu T, Nasahara KN. Why is chlorophyll b only used in light-harvesting systems? *Journal of Plant*  
389 *Research*. 2018;131(6):961-72.
- 390 30. Guo YY, Yu HY, Kong DS, Yan F, Zhang YJ. Effects of drought stress on growth and chlorophyll fluorescence of  
391 *Lycium ruthenicum* Murr. seedlings. *Photosynthetica*. 2016;54(4):524-31.
- 392 31. Yilmaz A, Rudolph HL, Hurst JJ, Wood TD. High-Throughput Metabolic Profiling of Soybean Leaves by Fourier  
393 Transform Ion Cyclotron Resonance Mass Spectrometry. *Analytical Chemistry*. 2016;88(2):1188-94.
- 394 32. Wei J, Li H, Barrow MP, O'Connor PB. Structural characterization of chlorophyll-a by high resolution tandem  
395 mass spectrometry. *J Am Soc Mass Spectrom*. 2013;24(5):753-60.
- 396 33. Wei J, O'Connor PB. Extensive fragmentation of pheophytin-a by infrared multiphoton dissociation tandem  
397 mass spectrometry. *Rapid communications in mass spectrometry : RCM*. 2015;29(24):2411-8.
- 398 34. He M, Ding N-Z. Plant Unsaturated Fatty Acids: Multiple Roles in Stress Response. *Frontiers in Plant Science*.  
399 2020;11(1378).

400 35. Routaboul JM, Fischer SF, Browse J. Trienoic fatty acids are required to maintain chloroplast function at low  
401 temperatures. *Plant Physiol.* 2000;124(4):1697-705.

402 36. Yaeno T, Matsuda O, Iba K. Role of chloroplast trienoic fatty acids in plant disease defense responses. *The*  
403 *Plant Journal.* 2004;40(6):931-41.

404  
405 All references should be numbered consecutively in order of appearance in main text, figures, tables and supplementary  
406 materials. References cited only in the supplementary materials should be listed at the end of the References section in  
407 main text. Citations of references in text should be identified using numbers in square brackets (e.g., “as discussed by  
408 [2]”; “as discussed elsewhere [2,3]”). The digital object identifier (DOI) should be included for all references where  
409 available.

410 Hapres uses “Vancouver” style, as outlined in the ICMJE sample references  
411 ([https://www.nlm.nih.gov/bsd/uniform\\_requirements.html](https://www.nlm.nih.gov/bsd/uniform_requirements.html)) with some variations on electronic materials.

How to cite this article:

Zemaitis KJ, Ye H, Nguyen HT, Wood TD. Direct Infusion Targeted Metabolomics of Phytochemicals in a  
Drought Tolerant Plant Introduction Soybean Cultivar. *Crop Breed Genet Genom.* 2020, submitted for  
review.